Journal of Forestry
https://doi.org/10.1007/s44392-026-00082-z

ORIGINAL PAPER

Frequency Versus Individual, Clumps, and Openings Prescription Marking: Comparison in Ponderosa Pine Restoration Treatments Using Uncrewed Aerial Systems

Wade T. Tinkham[1] · Mike A. Battaglia[1] · George A. Woolsey[2] · Lauren E. Lad[2] · Lance A. Asherin[1]

Received: 15 July 2025 / Accepted: 17 February 2026
This is a U.S. Government work and not under copyright protection in the US; foreign copyright protection may apply 2026

Abstract
Management of western United States dry-conifer forests has experienced a design shift from spacing-based treatments to maximize forest growth and minimize fire hazard towards balancing fuels reduction while restoring historical forest spatial patterns. However, successfully implementing spatially heterogeneous silvicultural treatments capable of mimicking a landscape's historical range of variability (HRV) has proven challenging. Early individual tree marking (ITM) strategies aiming to create heterogeneous forest structure often had unclear or confusing instructions. This study evaluates the ability of five ITM strategies to recreate HRV forest structure in Black Hills, South Dakota ponderosa pine forests. We started by first comparing uncrewed aerial system (UAS) derived forest inventory data against field plots and then assessing the UAS-derived tree spatial patterns of each ITM strategy against HRV. The UAS-detected trees were comparable to field plots providing an F-score averaging 0.943. The five ITM strategies created tree group size distributions that captured the range of individual trees and tree-clump-sizes but varied in their approximation of the HRV distribution. The individuals, clumps, and openings strategy and the two lowest cut-to-leave tree frequency strategies consistently matched four of five HRV group size metrics, while the other strategies typically only matched two or three metrics. Additionally, the frequency cut-to-leave tree strategy with 1:2 small-tree and 1:1 large-tree more often achieved all five HRV group size metrics compared to all other ITM strategies. Given the relatively even-aged starting forest structure from the stand's past management history, the lowest frequency cut-to-leave tree strategy provided the easiest to implement and most effective means of reproducing the HRV forest structure.

Keywords Silviculture · Restoration · Uncrewed aerial system · Individual tree detection · Spatial pattern

Extended author information available on the last page of the article

Introduction

Across many dry-conifer forests of the western United States there has been an increased emphasis on managing for complex forest structures to promote multiple management objectives (Hessburg et al. 2015; Addington et al. 2018; Stephens et al. 2021; Hagmann et al. 2021). Across most of these forests, fuel loading and forest density increased throughout the twentieth and twenty-first century from historical levels due to compounding fire suppression and land management decisions (Allen et al. 2002; Brown and Cook 2006; Battaglia et al. 2018; Johnston et al. 2018). This densification of dry-conifer forests has caused greater proportions of these landscapes, typically characterized as having historically frequent low and mixed-severity fires, to burn with greater proportions of high severity and across broader extents (Steel et al. 2015; Hagmann et al. 2021). Within these dry-conifer forest systems, forest treatments have largely shifted in design from optimizing forest growth through even spacing-based thinning to balancing fuels reduction while restoring forest spatial patterns (Larson and Churchill 2012; O'Hara and Nagel 2013). However, successfully implementing spatially heterogeneous silvicultural treatments capable of mimicking the historical range of variability seen in a landscape has proven challenging (Barrett et al. 2021; LeFevre et al. 2020).

These heterogeneous treatments, hereafter called restoration treatments, promote structural complexity by using spatially variable thinning to mimic the spatial heterogeneity of historical open forests comprised of openings, isolated individual trees, and groups of trees (Abella and Denton 2009; Larson and Churchill 2012). Recent studies have shown that when restoration treatments incorporate aspects of fuels management (Agee and Skinner 2005), such as some level of thinning from below and surface fuel treatment, these treatments can result in similar reductions in fire behavior and effects as targeted fuel hazard reduction treatments (Stephens et al. 2021; Ritter et al. 2022; Ziegler et al. 2025). Additionally, the complex forest structures resulting from restoration treatments promote a range of ecosystem services such as pollinator diversity (Rhoades et al. 2018), wildlife habitat (Reynolds et al. 2013; Latif et al. 2020), and understory plant diversity (Matonis and Binkley 2018; Demarest et al. 2023), producing a 600% return-on-investment in the most at-risk locations when considering a broad set of ecosystem services (Hjerpe et al. 2024). Restoration treatments often incorporate other prescription objectives beyond stand density and the spatial pattern of trees, such as species composition, tree size-class distribution, coarse woody debris, and dead standing snags. Commonly, the targets for residual forest structure and spatial patterns in restoration treatments are derived from an envelope of desired conditions based on historical reference stands, commonly called the historical range of variation (HRV; Franklin et al. 2013). These targets typically include a residual basal area and/or tree density as well as a distribution of residual trees or basal area within isolated individual trees and tree groups of various sizes (Churchill et al. 2016).

Spacing-based treatment designs of the late 20th and early twenty-first centuries prioritized optimizing forest growth and reducing fuel hazard by promoting an evenly spaced homogeneous residual forest structure (O'Hara and Nagel 2013; Underhill et al. 2014). This focus on homogeneity simplified treatment implementation, and facilitated widespread use, leading to well established forest management terminology and methods for homogeneous stand management. However, the subsequent shift toward promoting heterogeneity through restoration treatments created a period of inconsistent terminology use (Dickinson and Cadry 2017) and the development of several guides and tools to communicate the desired outcomes of restoration treatments (Churchill et al. 2016; Tinkham et al. 2017; Foppert et al. 2025).

Forest treatments use tree-marking strategies to communicate silvicultural prescriptions between those designing treatments to those implementing treatments. While the starting forest structure in a treatment unit influences the feasibility of meeting forest structural objectives through a single treatment (North and Sherlock 2012), the chosen marking strategy is equally crucial for effective treatment implementation (O'Hara et al. 2012). Restoration treatments commonly use either an Individual Tree Marking (ITM) or Operator Select marking strategy for implementation (Kellogg and Bettinger 1994; Yeo and Stewart 2000; Foppert et al. 2025). ITM strategies utilize a field crew to mark all trees for cutting or retention based on the silvicultural prescription, where it is more common to mark the leave-trees in restoration treatments due to their lower abundance compared to cut-trees (Forest Service 2009). The Operator Select system relies on either sawyers or equipment operators through either designation by description (DxD) or designation by prescription (DxP). With DxD, treatment implementors remove trees based on specific characteristics. In DxP, implementors use descriptions of desired outcomes to decide which trees to cut or retain while considering their spatial arrangement (Forest Service 2009).

Comparisons between the ITM and Operator Select approaches have shown that both can be equally effective at achieving desired forest structures regardless of whether spatial objectives are included (Kellogg and Bettinger 1994; Yeo and Stewart 2000; O'Hara et al. 2012; Dickinson and Cadry 2017; Foppert et al. 2025). However, success at achieving the desired outcomes varied with implementor experience. Interviews with restoration treatment operators have highlighted a preference for ITM over Operator Select approaches based on operator discomfort in selecting trees to achieve the treatment's intended targets (Dickinson and Cadry 2017). Conversely, when ITM strategy guidelines are unclear or confusing, field crews have been known to revert to simpler and easier to implement spacing-based strategies (O'Hara et al. 2012). Selection of tree-marking strategy and how it is communicated must consider tradeoffs in personnel experience and workload responsibility as these can be important considerations in achieving treatment outcomes (Foppert et al. 2025).

Prior assessments of marking strategies in restoration treatments have faced challenges fully evaluating differences in tree spatial arrangement due to limited availability of spatially continuous forest data. The existing literature uses proxies such as the coefficient of variation in tree size within sample plots (O'Hara et al. 2012) or tree canopy patch size (Dickinson and Cadry 2017) to describe tree-group-size distribution. However, recent advances in uncrewed aerial system (UAS) monitoring have enabled near-census level forest inventories of individual tree parameters at management unit scales (Belmonte et al. 2020). These UAS forest monitoring strategies have been successfully deployed for restoration treatment monitoring in ponderosa pine (*Pinus ponderosa* Lawson & C. Lawson var. *scopulorum* Englem.) and are reliably used to describe stand level forest densities and spatial arrangements (Hanna et al. 2024).

To address the challenges of ITM strategies becoming unclear or confusing when trying to generate heterogeneous forest structures, this study evaluates five ITM prescriptions of varying complexity. The objective is to determine the effectiveness of these prescriptions in creating forest structures indicative of the historical range of variation observed in Black Hills (South Dakota, USA) ponderosa pine forests. To achieve this, we collected UAS data and processed it to derive tree and plot level attributes, which were compared against field plots. Then using the UAS-derived near-census inventory, we evaluated how well each marking prescription recreated various metrics of the historical range of variation.

Methods

Study Area and Silvicultural Prescriptions

The study occurred in the Black Hills Experimental Forest, part of the Black Hills National Forest in South Dakota, United States (Fig. 1). Forests in the area are dominated by ponderosa pine with isolated groups of quaking aspen (*Populus tremuloides* Michx.) and paper birch (*Betula papyrifera* Marshall var. *papyrifera*) and scattered

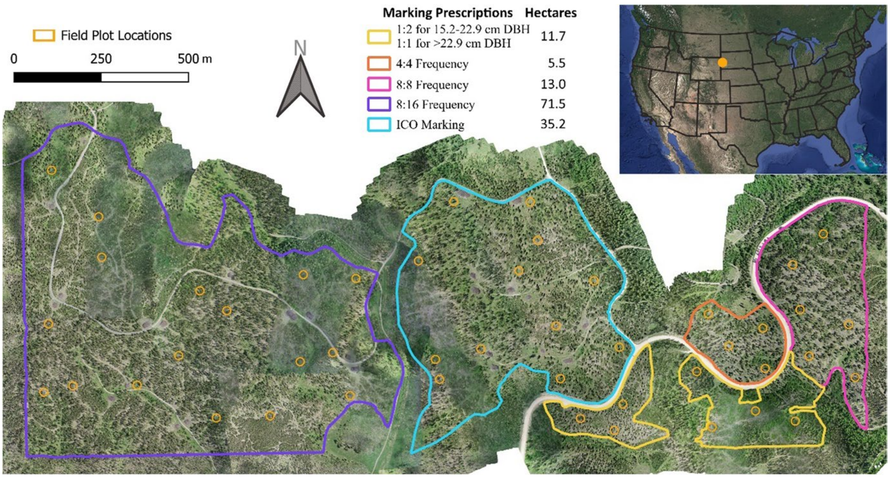

Fig. 1 Locations of the five silvicultural marking prescriptions in the Black Hills Experimental Forest, also shown in the inset map with an orange dot. Field plot locations for validating uncrewed aerial system observations are overlaid as orange circles, with background imagery derived from the DJI Phantom 4 Pro uncrewed aerial system collections. Marking prescriptions represent either a frequency ratio of cut vs retention trees or implementation of Individuals, Clumps, and Openings (ICO). All uncrewed aerial system imagery and field validation plot data are available through Tinkham et al. (2026)

individual white spruce (*Picea glauca* (Moench) Voss). Terrain slopes range from 0–30% with a mean of approximately 10%. Areas with established quaking aspen and paper birch were removed from study stands to isolate the assessment of ponderosa pine spatial arrangement. Stands were selected for having similar past management histories. Prior to implementation in 2021 of the silvicultural treatments analyzed in the present study, stands were last managed in 1991 and 1992 through either a shelterwood harvest or commercial thin of overstory trees in combination with a spacing-based thinning of advanced natural regeneration that established following individual-tree selection harvests in the 1950s (Boldt and Van Deusen 1974).

Prior to treatment, all stands had basal areas of 11.7 to 14.4 m^2 ha^{-1} (51.0 to 62.7 ft^2 $acre^{-1}$) for trees ≥ 15.2 cm (6 inch), with all stands having an average of 296 trees ha^{-1} (120 trees $acre^{-1}$) except for the stand receiving the Individual, Clumps, and Openings (ICO) treatment which averaged 213 trees ha^{-1} (86 trees $acre^{-1}$). For all except the ICO stand, there was an even split of pole size trees (15.2 cm to 22.9 cm; 6.0 inch to 9.0 inch) and sawlog size trees (≥ 22.9 cm; 9 inch) per hectare, with the pole size trees attributed to a combination of seedling establishment and regeneration release following the 1991 and 1992 treatments. However, the ICO stand had only about 10% of all trees in the pole size class.

The five ITM strategies were randomly assigned to study stands for the commercial removal of live ponderosa pine ≥ 15.2 cm diameter at breast height (DBH). The marking strategies each aimed to create a mosaic of tree groups (1 to 20 trees per group) by establishing a matrix of leave-tree groups and cut-tree groups to form openings. The silvicultural objective was to promote both horizontal and vertical heterogeneity, and for the resulting stand conditions to represent a clumpy/patchy horizontal distribution with varying tree DBHs and heights. All prescriptions were marked by Black Hills National Forest personnel in 2020 by walking each stand in parallel lines 20 m (66 ft) apart. All trees > 33 cm (13 inch) were retained, though these large trees were infrequent due to past management histories. In each ITM strategy, only the leave-trees were marked by the crew, with the crew instructed to select dominant and co-dominant size-class trees of good phenotypic characteristics as leave-trees (i.e. straight bole, crown ratio > 40%, healthy foliage, and good vigor).

The prescription intent was to recreate both stand densities and the distribution of isolated individual trees and tree groups of various sizes, with the targets for these values based on historical reconstruction plots from the Black Hills (Battaglia, unpublished data). See below for a description of how the historical reconstruction plots were collected and summarized. The four frequency marking prescriptions that were implemented included: 1) cut-to-leave tree ratios of 1:2 for 15.2 to 22.9 cm (6 to 9 inch) DBH and 1:1 for > 22.9 cm (9 inch) DBH; 2) 4:4 cut-to-leave tree; 3) 8:8 cut-to-leave tree; and 4) 8:16 cut-to-leave tree. During marking, individuals in the marking team alternated starting lines by designating trees as either cut or retain. For example, individuals in the 4:4 frequency mark would alternate skipping four trees for cutting and then mark four trees for retention. The rate and size of openings were not prescribed as part of the frequency marks, instead it was assumed that the cut and leave trees of different markers would randomly align to create both larger retention groups and produce openings of various sizes. The fifth ITM strategy sought to implement the Individual, Clumps, and Openings (ICO) prescription following Churchill et al. (2016). Marking progressed by first establishing 20 retention groups of 12 to 18 trees across the stand, followed by a multi-step spacing-based thinning of 7.6 m to 10.7 m (25 ft to 35 ft) between retention tree locations. The variation in distances was targeted to result in 87 to 173 tree locations (i.e. individuals or tree groups) per hectare. At 18 of these locations per hectare, 4 to 8 trees were marked for retention instead of just one, at 15 locations per hectare no trees were marked for retention to create small openings (radius ~ 15–21 m between trees), and at 10 locations per hectare an additional tree was set for removal to create large openings (radius ~ 30–42 m (98-138 ft) between trees). Trees were considered to be in a group if they were within 6 m (19.7 ft) stem-to-stem of another tree. The 6 m tree-to-tree distance represents the maximum crown size of mature trees to maintain interlocking crowns in the study area. This implementation of ICO required the marking crew to make repeated passes through the stand to establish different structures, while also tracking the frequency of different structures during the same pass. Following marking, stands were mechanically thinned using whole tree removal through skidding to designated landing areas.

Historical Range of Variation

The historical range of variation (HRV) for 1880 forest density and clumping arrangement was derived from 58 half hectare plots distributed across 10 sub-landscapes within the Black Hills of South Dakota (Battaglia, unpublished data). The sub-landscapes were developed to describe the distribution of soil and climatic variation across the Black Hills. The location of stand trees and remnant tree stumps/logs were recorded, and establishment dates were determined using methodologies similar to Brown et al. (2015) and Battaglia et al. (2018). These methods estimated tree DBH in 1880, which was used to quantify forest density and tree group arrangement for trees > 15.2 cm (6 inch) DBH. Tree group arrangements for the HRV data were determined following the methods developed and tested by Hanna et al. (2024). This process applies the density-based spatial clustering of applications with noise (DBSCAN) from the fpr package (Hahsler et al. 2019) in R to classify trees as being an isolated individual tree or as belonging to a tree group. Trees were assigned to a tree group if the tree-to-tree distance was ≤ 6 m (19.7 ft). Five classifications of tree groupings were then created: individual trees and tree groups of 2–4 trees, 5–9 trees, 10–15 trees, and > 15 trees.

Each HRV plot was summarized for trees and basal area per hectare, and then the proportion of trees and basal area was distributed to the five classes of tree groupings. From the individual HRV plots, the average for each sub-landscape was calculated for each metric, and an overall landscape interval for each metric was determined from the 10 sub-landscapes as the median plus and minus the standard deviation. This process resulted in a basal area interval of (median ± standard deviation) 18.60 ± 5.37 m^2 ha^{-1} (81.01 ± 23.39 ft^2 $acre^{-1}$), quadratic mean diameter of 36.6 ± 2.3 cm (14.4 ± 0.9 inch), and tree density of 164.0 ± 50.9 trees ha^{-1} (66.4 ± 20.6 trees $acre^{-1}$). The HRV plots showed a spatial distribution of structures with individual trees accounting for 18.4% ± 15.1% of all trees and groupings of 2–4 trees, 5–9 trees, 10–15 trees, and > 15 trees accounting for 30.9% ± 6.2%, 21.6% ± 7.4%, 9.6% ± 6.9%, and 18.2% ± 11.2% of all trees, respectively.

Validation Data Collection

To validate the UAS tree detection process, 46-0.04 ha (0.1 acre) circular plots were proportionally stratified to the marking strategies (Fig. 1). Plot locations were randomly generated, and plot centers were established in the field using an Emlid Reach RS2+real-time kinetic GPS with an average horizontal root mean squared error of 0.019 m (0.06 ft). In each plot, DBH, total height, distance from plot center, and azimuth from plot center were collected for all trees > 15.2 cm (6 inch) DBH, in alignment with the treatment prescriptions. During computation, individual trees were located based on the plot center coordinates and the tree distance and azimuth from plot center.

UAS Data Collection and Tree Detection

Imagery was collected using a DJI Phantom 4 Pro over a three-day period in May 2023. Flights were completed at 115 m (377 ft) above ground, using a 90% forward and 85% side image overlap, and flying at 6 m sec^{-1} (13.4 mph) resulting in imagery at 2.1 cm (0.83 inch) resolution (Fig. 2). Across the study extent, 115 ground control points were established at approximately one point per 1.5 hectares using an Emlid Reach RS2+real-time kinetic GPS with a reported horizontal root mean squared error of 0.027 m (0.89 ft). Imagery was processed using Agisoft Metashape Professional (Version 1.6.4; Agisoft LLC., St. Petersburg, Russia) following settings recommended in Tinkham and Woolsey (2024) for ponderosa pine dominated forests. A full table of processing settings for generating point clouds is available in supplemental Table S1. During processing, ground control points were identified in a minimum of 10 overlapping images, reporting alignment root mean squared errors for X, Y, and total horizontal of 6.0, 6.8, and 9.4 cm (2.4, 2.7, and 3.7 inch), respectively. The ground control points were included to minimize misalignment between UAS-detected trees and field inventoried trees. The resulting point cloud had > 800 points m^{-2} within treed areas.

Point clouds were processed using published methods (Swayze et al. 2021; Tinkham and Swayze 2021; Creasy et al. 2021; Swayze and Tinkham 2022) that utilize the lidR (Roussel et al. 2020) and lasR (Roussel 2025) packages of the R statistical program (R Core Team 2024). Point clouds had ground points identified using a cloth simulation filter (Zhang et al. 2016), noise points were filtered and removed, and the ground points were then used to height normalize the point cloud using a continuous digital terrain model (DTM) generated via Delaunay triangulation with linear interpolation within each triangle. The height normalized point cloud was then used to generate a canopy height model (CHM) at 0.2 m (0.66 ft) resolution using a point-to-raster local maximum approach and the St-Onge (2008) algorithm to fill pits and spikes in the raster.

Tree locations and heights were identified from the CHM using a variable window filter as implemented in Eq. 1.

$$Search\ Radius(m) = \begin{cases} 0.61.37 \leq CHM \leq 3 \\ 0.2 + (CHM \times 0.15)3 < CHM < 17 \\ 2.817 \leq CHM \end{cases} \tag{1}$$

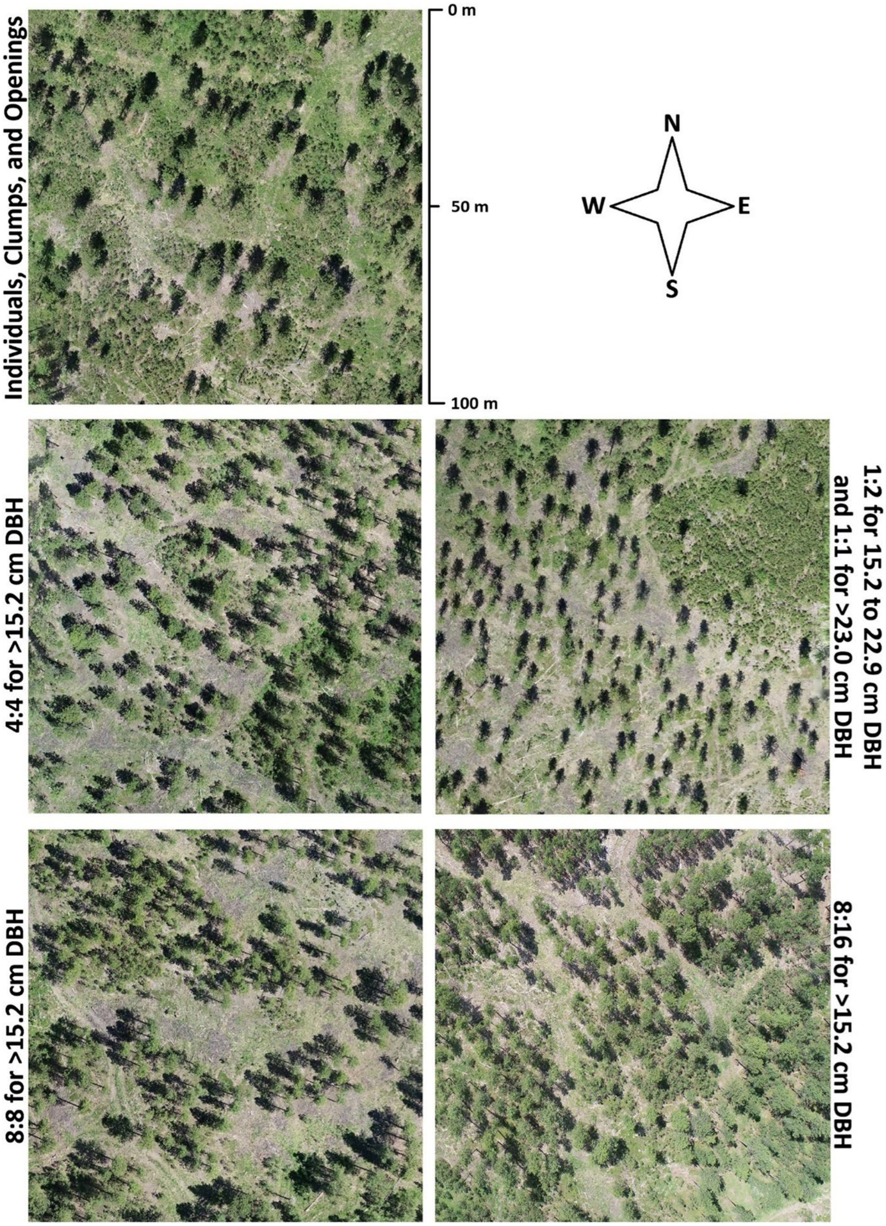

Fig. 2 Uncrewed aerial system orthomosaic imagery at 2.1 cm resolution showing a 1-hectare segment of each marking strategy following treatment

where *CHM* is the height in meters of an individual pixel from the canopy height model. This approach iterates over each CHM pixel, calculating the *Search Radius*, and identifies a tree if the focal pixel is the tallest pixel within the *Search Radius*.

The final parameters in Eq. 1 were set by iteratively inspecting UAS-detected tree locations on top of the CHM and UAS-derived orthomosaic of a 1-hectare subset to ensure the visual alignment of detected trees appearing to represent individual tree crowns.

Individual tree DBH values were estimated using a site-specific allometric equation developed from observations in the TreeMap dataset (Riley et al. 2021) within a 100 m (328 ft) buffer of the study area. TreeMap is a dataset of spatially imputed USDA Forest Service Forest Inventory and Analysis (FIA; Tinkham et al. 2018) plots. The allometries were fit using Eq. 2 with tree *Height* predicting *DBH* (Tinkham et al. 2022) and a zero intercept. The predictive model was fit using Bayesian modeling with a Gamma distribution and log link as implemented in the brms package (Bürkner 2017). The model was run with 4 chains, each chain had 4000 samples, with a warmup of 2000 samples and 8000 total post-warmup samples. The resulting relationship (Eq. 2) was used to predict a DBH for each UAS-detected tree. The final analysis dataset was filtered to only include UAS-detected trees with a DBH $\geq$ 15.2 cm (6 inch) to match the field-collected HRV and validation data. Processing of the structure from motion point cloud to a spatial forest inventory with location, height, and DBH for individual trees took 0.7 min ha^{-1} (0.28 min $acre^{-1}$).

$$DBH(cm) = 0 + b_1 \times Height(m) + Height(m)^{b_2} \tag{2}$$

Validation of UAS Tree Detection

The UAS-detected trees within each of the 0.04 ha (0.1 acre) validation plots were iteratively matched with the field-inventoried trees. Starting with the tallest individual field tree and working in descending height order, the process identified all UAS trees within a 3 m (9.8 ft) radius and within 2 m (6.6 ft) height of the field tree. If multiple UAS trees were identified, the tree closest in height was considered the True Positive match, and the resulting matched UAS and field tree were removed from further matching. When no UAS tree could be matched to a field tree, the field tree was classified as an Omission (i.e., False Negative). This process was repeated for all field trees with all unmatched UAS trees classified as Commissions (i.e., False Positives). Counts of trees in the confusion matrix were summarized as Recall (Eq. 3), Precision (Eq. 4), and F-score (Eq. 5). Where Recall is the rate of tree detection, Precision is a measure of detected tree correctness, and F-score is the method's overall accuracy, incorporating both precision and recall. The True Positive trees were further compared to the field trees they were matched against to determine the mean error and mean absolute error of tree height and DBH. Further, the UAS-detected trees in a plot were compared to the plot's field trees to determine the mean error and mean absolute error of trees per hectare and basal area per hectare.

$$Recall = \frac{True\ Positive}{True\ Positive + Commission} \tag{3}$$

$$Precision = \frac{True\ Positive}{True\ Positive + Omission} \tag{4}$$

$$F - score = 2 \times \frac{Recall \times Precision}{Recall + Precision} \tag{5}$$

Prescription Assessment

Tree groups in the UAS-detected data were classified using the same methods used for the HRV data (i.e., individual trees and tree groups of 2–4 trees, 5–9 trees, 10–15 trees, and > 15 trees). To compare the forest density and tree group arrangement resulting from the five marking strategies, we implemented 500 bootstrap samples with replacement to generate random plots equal to a 60% sampling intensity within the treatment area for each marking strategy. Circular 0.5 hectare (0.2 acre) plots were used to align with the plot size used during the HRV field data collection. Stand boundaries were inwardly buffered 5 m (16.4 ft) to minimize stand edge effects prior to sampling, when plots intersected the buffer, their plot radius was increased until the plot area within the buffered stand was a minimum of 0.495 hectares. Plot areas generated through this process were used to extract the UAS-detected trees for comparison against the HRV field data.

Within each sample plot, tree and tree group data was summarized using the same methods for HRV to describe trees and basal area per hectare, and the proportions distributed to individual trees and tree groups. Then, the plots within each marking strategy and individual bootstrap iteration were averaged, providing 500 bootstrap estimates of each metric for each marking strategy. For each marking strategy, each bootstrap iteration's average was evaluated for falling inside the HRV interval (median ± standard deviation). From this process, the proportion of bootstrap iterations within the interval were reported to represent the likelihood of the marking strategy generating a tree arrangement indicative of Black Hills HRV. Additionally, for the spatial arrangement metrics the mean and standard deviation of the five clumping metrics interval proportions (i.e., proportion of bootstrap samples inside the individual trees and tree groups of 2–4 trees, 5–9 trees, 10–15 trees, and > 15 trees intervals) are reported to describe the consistency in meeting all five spatial metrics.

Results

Tree Detection Accuracy

Evaluation of the UAS-detected trees against the 46 validation plots had an average F-score of 0.943 and 38 of the plots (83%) had an F-score > 0.93, with only four plots below 0.83 (Fig. 3). The high Precision measure approaching 100% achieved by the tree detection indicates that very few trees detected by the UAS could not be matched to a field tree. Visual inspection showed these Commission trees were located at the edge of the validation plots, suggesting the trees had enough lean that the tree top was inside the plot while the stem was rooted outside the plot. Plot-level Recall values which quantify the detection rate of validation sample trees were more varied (Fig. 3). This variation in Recall is attributed to the presence of smaller size class trees (15.24–20.32 cm DBH; 6.0 to 9.0 inch) which were potentially subdominant. A review of the 39 omitted trees across all plots showed that 22 trees (56%) were within 5 cm of the 15.2 cm minimum DBH threshold (2 inch of the 6 inch minimum). Additional inspection of all UAS-detected trees regardless of DBH, showed that each of these smaller Omission trees had a UAS-detected tree within a meter of it with a modeled DBH just below the minimum DBH threshold of 15.2 cm (6 inch).

For the True Positive matches, the UAS-detected tree heights had a mean error of −0.19 m (-0.62 ft) and mean absolute error of 0.48 m (1.57 ft), while tree DBHs had a mean error of −1.5 cm (-0.6 inch) and a mean absolute error of 2.7 cm (1.06 inch). When propagating the tree detection errors to the hectare level, there was an underestimate by the UAS of 11%, but ignoring the Omission trees within 5 cm (2 inch) of the minimum DBH threshold would reduce the underestimation to 4.2%. The under detection of trees and underestimation bias in the UAS modeled DBH values compound and propagate through to the UAS basal area per hectare having an underestimation of 16.3%.

Marking Strategy Assessment

Assessment of the post-treatment stand density based on UAS-detected trees reveals that, while some bootstrap samples for all five ITM strategies fell within the HRV interval for trees per hectare, the frequency of this varied widely across marking strategies (Fig. 4). The percentage of bootstrap samples within the HRV interval substantially decreased from ~ 100% for the ICO and 1:2/1:1 marking approaches to only 0.8% for the 8:16 frequency marking approach. The coefficient of variation in post-treatment trees per hectare within each marking strategies

Fig. 3 Summary of the tree extraction quality from the 46 validation plots

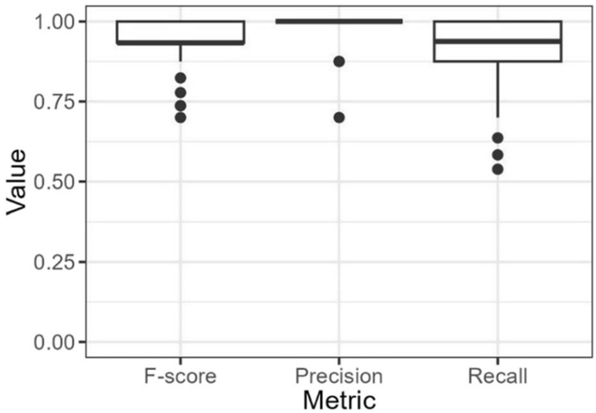

was lowest for the ICO (4.7%), 8:8 (4.6%), and 8:16 (4.0%) frequency marking approaches, while the 1:2/1:1 (9.8%) and 4:4 (7.3%) marking frequencies were more variable.

Quantification of the post-treatment spatial arrangement revealed that all marking strategies achieved some level of overlap with the five HRV clumping metrics (Fig. 5). However, the extent to which each strategy replicated the HRV varied. This variation was observed both between different marking strategies for a single clumping metric and across the five clumping metrics for any given marking strategy. As the cut-to-leave tree ratio increased, the representation of larger clumps (> 15 tree groups) also increased while smaller tree clumps (individuals and 2–4 tree groups) were underrepresented compared to HRV (Fig. 5). The ICO and 1:2/1:1 marking strategies had a higher proportion of individuals and 2–4 tree groups within the HRV interval and a lower proportion of > 15 tree groups compared to the 8:8 and 8:16 marking frequency approaches which showed the opposite pattern. Overall, similar trends were observed for the proportion of basal area distributed across the five clumping group (data not shown).

Overall, the ICO, 1:2/1:1, and 4:4 marking strategies maintained a higher average proportion of bootstrap samples within the HRV intervals across the five clumping metrics for both trees per hectare and basal area. However, there was greater variability between these metrics for the ICO marking strategy compared to the 1:2/1:1 and 4:4 frequency strategies (Table 1). Conversely, the 8:8 and 8:16 frequency marking strategies had substantially lower average success at achieving outcomes within the HRV intervals, and higher variability in success rates (ranging from < 10% to 100%) across the five metrics (Figs. 4 and 5). Evaluating the number of metrics that an individual bootstrap sample fell within the HRV interval shows that the ICO, 1:2/1:1, and 4:4 marking strategies all achieved four out of five clumping metrics roughly 80% of the time (Fig. 5). However, these strategies differed in their ability to achieve all five metrics, with the 1:2/1:1 marking strategy doing so in > 50% of samples, ICO around 35%, and 4:4 around 25%. Conversely, achieving all five metrics or even four of the five metrics with the 8:8 and 8:16 marking strategies was rare (Fig. 6).

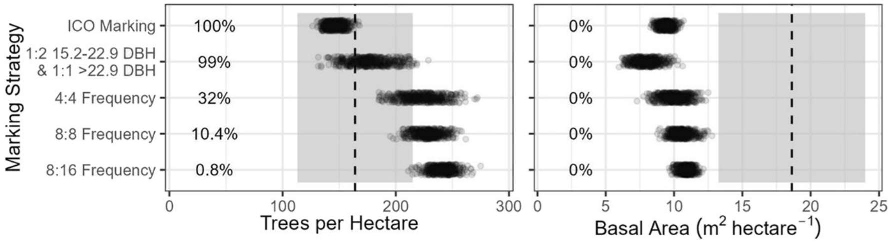

Fig. 4 Distribution of trees per hectare and basal area (trees > 15.2 cm DBH; 6 inch) from the bootstrap samples of the five marking strategies compared to the historical range of variability. The dashed lines and grey bands represent the median and ± 1 standard deviation of each metric's historical range of variability. Each dot represents one of the 500 bootstrap samples, while inset values to the left report the percentage of bootstrap samples inside the historical range of variability

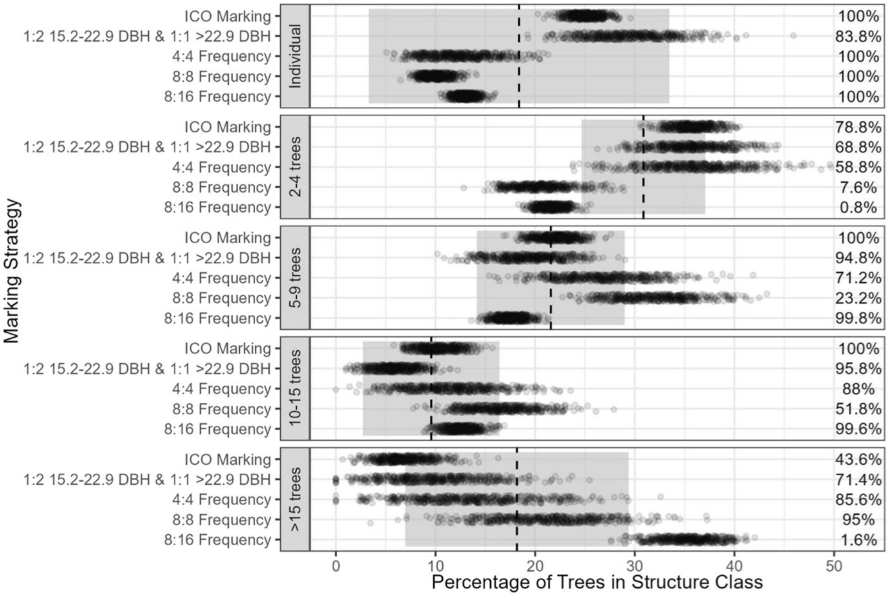

Fig. 5 Distribution of percent of trees (trees > 15.2 cm DBH; 6 inch) in different tree group sizes from the bootstrap samples of the five marking strategies compared to the historical range of variability. The dashed vertical lines and grey bands represent the median and ± 1 standard deviation of a metric's historical range of variability. Each dot represents one of the 500 bootstrap samples and inset values report the percentage of bootstrap samples inside the historical range of variability

Table 1 Summary of the proportion of bootstrap samples from each marking strategy that fell inside the historical range of variability. The mean, standard deviation (SD), min, and max represent the distribution for the five clumping metrics

Marking Strategy	% Trees in Clump Size				% Basal Area in Clump Size			
	Mean	SD	Min	Max	Mean	SD	Min	Max
ICO Marking	84.5	24.6	43.6	100.0	80.5	30.0	31.8	100.0
1:2 15.2–22.9 DBH & 1:1 > 22.9 DBH	82.9	12.6	68.8	95.8	80.8	16.8	58.0	96.4
4:4 Frequency	80.7	16.0	58.8	100.0	77.4	22.4	40.8	100.0
8:8 Frequency	55.5	41.5	7.6	100.0	52.4	42.8	8.2	100.0
8:16 Frequency	60.4	54.0	0.8	100.0	59.6	53.9	0.2	100.0

Discussion

Comparison of Marking Strategies

The study tested the ability of five individual tree marking (ITM) strategies to recreate spatial structures representative of the historical range of variation (HRV), including ICO, 1:2/1:1, 4:4, 8:8, and 8:16 for trees > 15.2 cm (6.0 inch) DBH. The

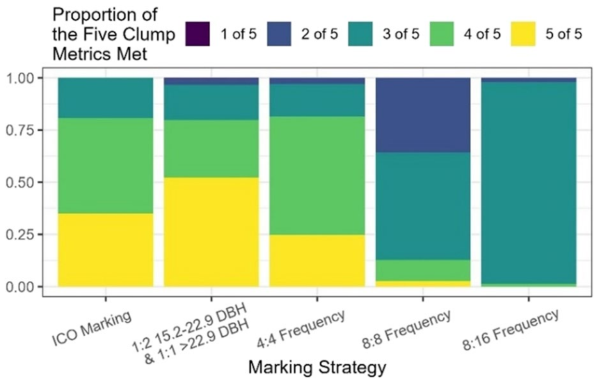

Fig. 6 The proportion of the 500 bootstrap samples in each marking strategy that fell inside the historical range of variability for one to five clumping metrics (e.g., for ICO Marking, ~ 36% of the bootstraps met all five metrics simultaneously (yellow section of bar)). Each of the 500 bootstrap samples in a stand were evaluated for simultaneously falling inside the historical range of variation intervals for individual trees and the various tree-group sizes (e.g., a single bootstrap sample might only fall inside 3 of 5 intervals)

ICO strategy represents the most complex and time consuming to implement strategy with the marking crew making multiple passes through the treatment unit to first select large clumps for retention and then selecting spacing-based locations to establish the retention of individual trees, small clumps of trees, and small openings. Conversely, the frequency marking strategies had the crew alternating between skipping trees to be cut and marking trees for retention during a single pass through the stand, where the cut-to-leave tree ratios for the 1:2/1:1 strategy were 1:2 for 15.2 to 22.9 cm (6.0 to 9.0 inch) DBH and 1:1 for > 22.9 cm (9.0 inch) DBH.

Evaluation of the five marking strategies shows the ICO, 1:2/1:1, and 4:4 strategies (from least to most complex) have a high probability of providing a reasonable approximation of the HRV intervals for the distribution of trees and basal area within different clump sizes. Conversely, the 8:8 and 8:16 frequency marking strategies typically only achieved outcomes within the HRV interval for three of the five clumping metrics. Additionally, while both the ICO and 1:2/1:1 marking strategies frequently produced forest structures within the HRV interval for trees per hectare, the 1:2/1:1 strategy created greater within stand density variability as it resulted in a coefficient of variation for trees per hectare twice that of the ICO approach, but with nearly all of the bootstrap samples still falling inside the HRV interval. The effectiveness of these marking strategies to produce forest structures resembling the HRV must be evaluated considering past management history. The historical emphasis on timber production in these stands likely explains why simultaneous achievement of the trees per hectare and basal area per hectare HRV was not observed. Our UAS data estimated quadratic mean diameters ranging from 23.9 cm to 28.8 cm (9.4 inch to 11.3 inch) across the five stands, whereas the HRV data showed a median quadratic mean diameter of 36.6 cm (14.4 inch). This difference in tree size between the contemporary stands and the HRV data likely represents 10–15 years of growth in the study stands (Tinkham et al. 2021) but is also why the prescriptions were designed to achieve a trees per hectare objective but could not simultaneously represent the HRV basal area or quadratic mean diameter at this time.

The five marking strategies in this study represented a range of marking complexity and time requirement, which is inversely related to the ease of field implementation. Overall, the 1:2/1:1 frequency marking strategy appeared to best balance creating stand-level heterogeneity while being easy for markers to understand and efficiently implement (personal communication with marking team). This marking approach not only met the target trees per hectare, but also created substantial within-stand trees per hectare variability and more often achieved results within all five HRV clumping metrics compared to the other strategies (Fig. 6). Our finding of a marking strategy that successfully recreates aspects of the HRV while being easily implemented by markers differs from previous assessments trying to identify simple marking strategies for promoting heterogeneity. For example, O'Hara et al. (2012) compared six marking strategies and found that only the most complex strategies (i.e. ICO) could create within-stand heterogeneity, while simpler marking strategies were less effective at enhancing structural complexity. Similarly, Maher et al. (2019) found that the ICO marking strategy produced tree densities closer to the prescription and enhanced heterogeneity compared to a simpler free selection marking strategy.

The implementation of the ICO marking strategy tested in this study, based on Churchill et al. (2016), successfully generated a range of clump sizes similar to the HRV, achieving four of the five clumping metrics in over 80% of the bootstrap samples (Fig. 6). While the ICO strategy also met the HRV target for trees per hectare, it simultaneously produced the lowest level of within-stand variability in trees per hectare (Fig. 4). However, the ICO implementation may have been hindered by having the lowest starting stand density of all study stands. This low starting stand density likely resulted in the implementation creating a higher proportion of isolated individual trees and 2–4 tree groups than was typical in the HRV. Implementing the ICO strategy in a stand with a higher starting stand density should allow it to create more > 15 tree groups and increase the within-stand trees per hectare variability by creating areas with both higher density and larger openings. The ICO strategy might achieve similar ease of implementation as the 1:2/1:1 frequency marking strategy, with prior work showing that marking crews found individual tree marking prescriptions easier to implement when using integrated field tablets with real-time tracking of prescription targets (Maher et al., 2019).

The 1:2/1:1 and ICO marking strategies provided close approximations of the HRV intervals but differed slightly in their distribution of group sizes with the 1:2/1:1 strategy promoting more individual trees and 2–4 tree groups, while ICO had a slightly greater representation of 5–9 tree and 10–15 tree groups (Fig. 5). Selecting between these small shifts in the distribution of group sizes could better align with local management priorities, however, these differences are as likely to occur due to starting stand conditions as how the marking strategies were implemented. Ultimately, managers must use a sense of place in the broader landscape to balance multiple resource objectives that can be at odds with each other when it comes to the forest structure best suited to meet place specific objectives. With HRV in this landscape providing a range of individual trees from ~ 3% to 33% of all trees, managers have flexibility to design treatments that might prioritize specific disturbance patterns or ecosystem services in different parts of a landscape, while providing both within and between stand scales of heterogeneity. Physics-based fire modeling of restoration treatments has shown that promoting higher proportions of individual trees and small tree groups can reduce canopy consumption during fires (Ziegler et al. 2025). Conversely, it is known that the presence of large tree groups with high canopy cover represents critical habitat for Northern goshawk (*Accipiter gentilis*) nesting and roosting, with the bird requiring this close to the more open forest conditions they use for hunting (Reynolds et al. 1992). While stand-level decisions must be made to balance objective priorities, at the landscape scale, promoting greater forest structural and compositional heterogeneity has been shown to benefit overall forest resilience to drought, fire, and bark beetle disturbance events (Young et al. 2017). It is widely documented that historical forest structures varied both within and between landscapes, to introduce the broader scale of heterogeneity, managers could consider varying marking frequencies across environmental conditions.

Influence of UAS Tree Detection

The UAS tree detection process in this study achieved high accuracy, with an average F-score of 0.943, especially when compared with other studies in ponderosa pine forests (0.64 to 0.94; Hanna et al. 2024; Mohan et al. 2017; Silva et al. 2016). Evaluation of plots with higher omission errors showed that these errors were most common in stands treated with the 8:8 and 8:16 marking strategies (72% of omitted trees), specifically in areas of denser tree clumps. This tendency for greater omission errors in higher density areas has been observed in other studies, where intermediate and suppressed trees account for the majority of omitted trees (Creasy et al. 2021). In our study, a significant portion (56%) of the trees undetected using the UAS approach were within 5 cm (2 inch) of the 15.2 cm (6 inch) DBH inclusion threshold. Visual inspection confirmed that a tree was detected by the UAS method at each of these locations, but the modeled DBH was just below the threshold for inclusion. Additionally, another 10% of the missed trees from the UAS method were recorded to have a broken top, which caused their detected heights to fall below the threshold required for inclusion based on the height-DBH model. These findings indicate that while the DBH modeling process provides a reasonable approximation, tree structural defects or local conditions that deviate from the expected height-to-DBH relationship can introduce errors which potentially propagate through to subsequent analysis, with this likely being more common in pre-treatment conditions.

The slight underestimation of tree density by the UAS method likely extends to the estimated trees per hectare and potentially influences the observed distribution of tree clump sizes. Given that most omitted trees occurred within the larger tree clumps of the 8:8 and 8:16 marking strategies, the overrepresentation of 10–15 tree and > 15 tree clumps in our data may be even more pronounced in reality. However, since the majority of plots with omitted trees occurred within the 8:8 and 8:16 marking strategies, the structural heterogeneity described by the UAS data for the ICO and 1:2/1:1 strategies is likely more reliable. The high fidelity of UAS-detected trees in post-treatment open-canopy ponderosa pine forests aligns with prior research (Belmonte et al. 2020; Hanna et al. 2024).

As UAS technology matures and field tablets with integrated GPS become more accurate, the near-census forest inventories achievable through UAS methods could streamline implementation of heterogeneous treatments by directly connecting data collection with marking practices. LiDAR-derived individual tree inventories have been successfully used to compare alternative treatment strategies and enable the implementation of optimal treatments in the field (Wing et al. 2019). These remotely sensed forest inventories, often referred to as “digital-twins”, can then be readily transferred to field tablets for marking crews or even directly utilized by harvest equipment operators to execute treatments effectively (Keefe et al. 2022). Hybrid implementation strategies that borrow principals from both ITM and DxP, becoming known as DxP+, are emerging for spatially complex prescriptions. These DxP+approaches use remote sensing data to delineate groups of leave-trees and how many trees to retain in the grouping but leaves the tree-level selection to the harvest operator (Foppert et al. 2025). Early evaluation of these approaches has seen a 10- to 15-fold reduction in implementation cost without any change in implementation efficiency (Foppert et al. 2025). Further work is needed to develop strategies for this technology’s integration and to evaluate its influence on treatment implementation efficiency and effectiveness.

Transferring Findings

The ponderosa pine forests of the Black Hills commonly exhibit regeneration densities far exceeding other ponderosa pine regions due to prolific seed crops and favorable summer precipitation patterns (Oliver and Ryker 1990). These abundant seed crops occur every 2–5 years and commonly result in more than 5,000 trees ha^{-1} (1,969 trees $acre^{-1}$) successfully establishing (Shepperd and Battaglia 2002). It is likely the pole size trees (15.2 cm to 22.9 cm; 6.0 inch to 9.0 inch) in the pre-treatment inventory, representing about half of all trees > 15.2 cm (6 inch) in each stand, developed from a mixture of advanced regeneration being released following the 1991/1992 treatments or subsequent regeneration. The ability for these Black Hills forests to so quickly regenerate likely makes the legacy of spacing-based thinning management history have less impact on the ability to promote spatial heterogeneity in these stands, with the rapid ingrowth providing options for manipulating a stand’s spatial pattern. However, other silvicultural systems like commercial thinning and free selection within the Black Hills have been shown to fail to promote heterogeneity similar to HRV, with Ritter et al. (2022) finding these treatments resulted in 69% to 77% individual trees, 22% to 28% 2–4 tree groups, and very limited larger groups.

Translating how these marking strategies performed in the Black Hills to forests with more sporadic regeneration patterns, to restore heterogeneity in stands previously managed using spacing-based thinning could prove challenging. Without the abundant regeneration seen in the Black Hills, there may not be a high enough stand density in the necessary size classes for the 1:2/1:1 marking frequency to still produce the 5–9 tree and 10–15 tree groups. In these conditions, alternative frequency marking ratios of cut-to-leave trees may need to be explored, or it may be necessary to have marking crews alternate between two frequencies like 2:3 and 8:8 in adjacent lines to create the desired heterogeneity. Additionally, restoring stands previously managed with spacing-based thinning may require multiple management actions over time to enhance heterogeneity through an iterative approach. Ideally, follow up precommercial thinning in these stands can consider the locations of advanced regeneration and established overstory trees to promote clumps of varying group sizes and tree sizes. The integration of UAS tree-level monitoring through time could provide the necessary spatial data for tracking forest structure spatial heterogeneity through repeated stand entries to balance multiple objectives.

Management Applications

Our evaluation of five individual tree marking strategies indicates the ICO and 1:2/1:1 and 4:4 frequency marking strategies had similarly high likelihoods of creating a reasonable representation of HRV. However, the 1:2/1:1 strategy most consistently met the desired distribution of clump sizes and within-stand variation in trees per hectare compared to the other methods. Furthermore, this low-frequency marking strategy presents an easy to implement alternative to more complex marking strategies for introducing heterogeneity into stands previously managed under spacing-based, even-aged systems. While the 1:2/1:1 frequency marking was the most effective at promoting heterogeneity in stands previously managed through spacing-based thinning for timber production, this success is at least partially attributed to the high regeneration density within the Black Hills providing enough candidate trees for the markers to select from. This study also highlights the potential of uncrewed aerial systems (UAS) for monitoring and assessing forest structure and spatial arrangement, particularly in lower canopy cover forests (i.e., $<70\%$ canopy cover). To better translate these findings into management practice, future research should focus on further trials of frequency marking in stands with diverse management histories to enhance our understanding of how these histories interact with the cut-to-leave tree ratios. Additionally, exploration of the use of UAS-based forest inventories to aid in stand marking needs to be explored for the potential efficiency gains it could provide.

Supplementary Information The online version contains supplementary material available at https://doi.org/10.1007/s44392-026-00082-z.

Acknowledgements We would like to thank the dedicated marking crew from the Black Hills National Forest who implemented these treatments, making this project possible. The findings and conclusions in this publication are those of the authors and should not be construed to represent any official US Department of Agriculture or US Government determination or policy.

Author Contributions Wade Tinkham and Mike Battaglia contributed to the conception and design of the study. Mike Battaglia and Lance Asherin designed the silvicultural treatments and worked with the Black Hills National Forest on their implementation. Wade Tinkham, George Woolsey, and Lauren Lad collected the field observations and uncrewed aerial system (UAS) data. George Woolsey and Wade Tinkham processed the UAS data. Wade Tinkham performed the statistical analysis. All authors provided input about data interpretation. Wade Tinkham wrote the first draft of the manuscript. Mike Battaglia, George Woolsey, Lauren Lad and Lance Asherin contributed to the manuscript revision. All authors read and approved the submitted version.

Funding This research was supported by funding from the US Department of Agriculture's National Institute of Food and Agriculture program (2022–67021-37857) and USDA Forest Service with funding from the Bipartisan Infrastructure Law. This research was supported by the USDA Forest Service, Rocky Mountain Research Station.

Data Availability All data used in this study is available through the USDA Forest Service Data Archive at https://doi.org/10.2737/RDS-2026-0003

Declarations

Competing interests The authors declare that they have no known competing financial interests or personal relationships that could have appeared to influence the work reported in this paper.

Open Access This article is licensed under a Creative Commons Attribution 4.0 International License, which permits use, sharing, adaptation, distribution and reproduction in any medium or format, as long as you give appropriate credit to the original author(s) and the source, provide a link to the Creative Commons licence, and indicate if changes were made. The images or other third party material in this article are included in the article's Creative Commons licence, unless indicated otherwise in a credit line to the material. If material is not included in the article's Creative Commons licence and your intended use is not permitted by statutory regulation or exceeds the permitted use, you will need to obtain permission directly from the copyright holder. To view a copy of this licence, visit http://creativecommons.org/licenses/by/4.0/.

References

Addington, R.N., Aplet, G.H., Battaglia, M.A., Briggs, J.S., Brown, P.M., Cheng, A.S., Dickinson, Y.L., Feinstein, J.A., Pelz, K.A., Regan, C.M., Thinnes, J., Truex, R., Fornwalt, P.J., Gannon, B., Julian, C.W., Underhill, J.L., Wolk, B. 2018. Principles and practices for the restoration of ponderosa pine and dry mixed-conifer forests in the Colorado Front Range. General Technical Report RMRS-GTR-373. USDA Forest Service Rocky Mountain Research Station. Fort Collins, CO.

Agee, J. K., and C. N. Skinner. 2005. Basic principles of forest fuel reduction treatments. *Food Policy* 211:83–96. https://doi.org/10.1016/j.foreco.2005.01.034.

Allen, S. R., M. Savage, D. A. Falk, K. F. Suckling, T. W. Swetnam, T. Shulke, P. B. Stacey, P. Morgan, M. Hoffman, and J. T. Klingel. 2002. Ecological restoration of southwestern ponderosa pine ecosystems: A broad perspective. *Ecological Applications* 12:1418–1433. https://doi.org/10.1890/1051-0761(2002)012[1418:EROSPP]2.0.CO;2.

Barrett, K. J., J. B. Cannon, A. M. Schuetter, and A. S. Cheng. 2021. Effects of collaborative monitoring and adaptive management on restoration outcomes in dry conifer forests. *Food Policy* 488:119018. https://doi.org/10.1016/j.foreco.2021.119018.

Battaglia, M. A., B. Gannon, P. M. Brown, P. J. Fornwalt, A. S. Cheng, and L. S. Huckaby. 2018. Changes in forest structure since 1860 in ponderosa pine dominated forests in the Colorado and Wyoming Front Range, USA. *Forest Ecology and Management* 422:147–160. https://doi.org/10.1016/j.foreco.2018.04.010.

Belmonte, A., T. Sankey, J. A. Biederman, J. Bradford, S. J. Goetz, T. Kolb, and T. Woolley. 2020. UAV-derived estimates of forest structure to inform ponderosa pine forest restoration. *Remote Sensing in Ecology and Conservation* 6 (2): 181–197. https://doi.org/10.1002/rse2.137.

Boldt, C.E., Van Deusen, J.L. 1974. Silviculture of ponderosa pine in the Black Hills: The status of our knowledge. Research Paper RM-RP-124. Fort Collins, CO: USDA Forest Service, Rocky Mountain Forest and Range Experiment Station. 45 p.

Brown, P. M., and B. Cook. 2006. Early settlement forest structure in Black Hills ponderosa pine forests. *Forest Ecology and Management* 223 (1–3): 284–290.

Brown, P. M., M. A. Battaglia, P. J. Fornwalt, B. Gannon, L. S. Huckaby, C. Julian, and A. S. Cheng. 2015. Historical (1860) forest structure in ponderosa pine forests of the northern Front Range Colorado. *Canadian Journal of Forest Research* 45:1462–1473. https://doi.org/10.1139/cjfr-2014-0387.

Bürkner, P.-C. 2017. brms: An R package for Bayesian multilevel models using Stan. *Journal of Statistical Software* 80:1–28.

Churchill, D.J., Larson, A.J., Jeronimo, S.M.A., Fischer, P.W., Dalhgreen, M.C., Franklin, J.F. 2016. The ICO approach to quantifying and restoring forest spatial pattern: Implementation guide. Version 3.0 Stewardship Forestry and Science, Vashon, Washington, USA.

Creasy, M. B., W. T. Tinkham, C. M. Hoffman, and J. C. Vogeler. 2021. Potential for individual tree monitoring in ponderosa pine dominated forests using unmanned aerial system structure from motion point clouds. *Canadian Journal of Forest Research* 51:1093–1105. https://doi.org/10.1139/cjfr-2020-0433.

Demarest, A. B., P. J. Fornwalt, B. H. Wolk, K. C. Rodman, and M. D. Redmond. 2023. Mechanical forest restoration treatments stimulate understory plants in the Colorado Front Range. *Forest Ecology and Management* 548:121322. https://doi.org/10.1016/j.foreco.2023.121322.

Dickinson, D. L., and J. D. Cadry. 2017. An evaluation of tree marking methods for implementing spatially heterogeneous restoration. *Journal of Sustainable Forestry* 36 (1): 47–64. https://doi.org/10.1080/10549811.2016.1251325.

Foppert, J. D., N. F. Maker, K. M. Waring, T. Woolley, M. R. Nabel, J. Rainey, and J. A. Jurgens. 2025. Innovative tree designation methods for a complex silvicultural treatment: Costs, efficiency and outcomes. *Journal of Forestry* 123:781–800. https://doi.org/10.1007/s44392-025-00051-y.

Franklin, J. F., N. K. Johnson, D. J. Churchill, K. Hagmann, D. Johnson, and J. Johnston. 2013. *Restoration of dry forests in Eastern Oregon: A field guide*. Portland, OR: The Nature Conservancy of Oregon.

Hagmann, R.K., Hessburg, P.F., Prichard, S.J., Povak, N.A., Brown, P.M., Fule, P.Z., Keane, R.E., Knapp, E.E., Lydersen, J.M., Metlen, K.L., Reilly, M.J., Sanchez Meador, A.J., Stephens, S.L., Stevens, J.T., Taylor, A.H., Yocom, L.L. Battaglia, M.A., Churchill, D.J., Daniels, L.D., Falk, D.A., Henson, J.D., Johnston, M.A., Krawchuk, Levine, C.R., Meigs, G.W., Merschel, A.G., North, M.P., Safford, H.D., Swetnam, T.W., Waltz, A.E.M. 2021. Evidence for widespread changes in the structure, composition, and fire regimes of western North American forests. *Ecological Applications* 31(8): e02431. https://doi.org/10.1002/eap.2431.

Hahsler, M., Piekenbrock, M., Doran, D. 2019. dbscan: Fast density-based clustering with R. *Journal of Statistical Software* 91(1). https://doi.org/10.18637/jss.v091.i01.

Hanna, L., W. T. Tinkham, M. A. Battaglia, J. C. Vogeler, S. M. Ritter, and C. M. Hoffman. 2024. Characterizing heterogeneous forest structure in ponderosa pine forests via UAS-derived structure from motion. *Environmental Monitoring and Assessment* 196 : 530. https://doi.org/10.1007/s10661-024-12703-1.

Hessburg, P. F., D. J. Churchill, A. J. Larson, R. D. Haugo, C. Miller, T. A. Spies, and G. H. Reeves. 2015. Restoring fire-prone Inland Pacific landscapes: Seven core principles. *Landscape Ecology* 30:1805–1835. https://doi.org/10.1007/s10980-015-0218-0.

Hjerpe, E. E., Colavito, M. M., Waltz, A. E. M., Sanchez Meador, A. 2024. Return on investment in restoration and fueltreatments in frequent-fi re forests of the American west: a meta-analysis. *Ecological Economics* 223:108244. https://doi.org/10.1016/j.ecolecon.2024.108244.

Johnston, J. D., C. J. Dunn, M. J. Vernon, J. D. Bailey, B. A. Morrissette, and K. E. Morici. 2018. Restoring historical forest conditions in a diverse inland Pacific Northwest landscape. *Ecosphere* 9 (8): e02400.

Keefe, R. F., E. G. Zimbelman, and G. Picchi. 2022. Use of individual tree and product level data to improve operational forestry. *Current Forestry Reports* 8:148–165. https://doi.org/10.1007/s40725-022-00160-3.

Kellogg, L. D., and P. Bettinger. 1994. Thinning productivity and cost for a mechanized cut-to-length system in the Northwest Pacific Coast region of the USA. *Journal of Forest Engineering* 5 (2): 43–54. https://doi.org/10.1080/08435243.1994.10702659.

Larson, A. J., and D. Churchill. 2012. Tree spatial patterns in fire-frequent forests of western North America, including mechanisms of pattern formation and implications for designing fuel reduction and restoration treatments. *Forest Ecology and Management* 267:74–92. https://doi.org/10.1016/j.foreco.2011.11.038.

Latif, Q. S., R. L. Truex, R. A. Sparks, and D. C. Pavlacky Jr. 2020. Dry conifer forest restoration benefits Colorado Front Range avian communities. *Ecological Applications*. https://doi.org/10.1002/eap.2142.

LeFevre, M. E., D. J. Churchill, A. J. Larson, S. M. Jeronimo, J. Bass, J. F. Franklin, and V. R. Kane. 2020. Evaluating restoration treatment effectiveness through a comparison of residual composition, structure, and spatial pattern with historical reference sites. *Forest Science* 66 (5): 578–588.

Maher, C. T., E. Oja, A. Marshall, M. Cunningham, L. Townsend, G. Worley-Hood, L. R. Robinson, T. Margot, D. Lyons, S. Fety, E. E. Schneider, S. M. A. Jeronimo, D. J. Churchill, and A. J. Larson. 2019. Real-time monitoring with a tablet app improves implementation of treatments to enhance forest structural diversity. *Journal of Forestry* 3:280–292. https://doi.org/10.1093/jofore/fvz003.

Matonis, M. S., and D. Binkley. 2018. Not just about the trees: Key role of mosaic-meadows in restoration of ponderosa pine ecosystems. *Forest Ecology and Management* 411:120–131. https://doi.org/10.1016/j.foreco.2018.01.019.

Mohan, M., Silva, C. A., Klauberg, C., Jat, P., Catts, G., Cardil, A., Hudak, A.T., Dia, M. 2017. Individual tree detectionfrom unmanned aerial vehicle (UAV) derived canopy height model in an open canopy mixed conifer forest. *Forests* 5(9):340. https://doi.org/10.3390/f8090340.

North, M., Sherlock, J. 2012. Chapter 9: Marking and assessing forest heterogeneity. *In: North, Malcolm, ed. 2012.Managing Sierra Nevada forests. Gen. Tech. Rep. PSW-GTR-237. Albany, CA: USDA Forest Service, Pacific Southwest Research Station. pp. 95-105*. https://research.fs.usda.gov/treesearch/41089.

O'Hara, K. L., and L. M. Nagel. 2013. The stand: Revisiting a central concept in forestry. *Journal of Forestry* 111 (5): 335–340.

O'Hara, K. L., L. P. Leonard, and C. R. Keyes. 2012. Variable-density thinning and a marking paradox: Comparing prescription protocols to attain stand variability in coast redwood. *Western Journal of Applied Forestry* 27 (3): 143–149. https://doi.org/10.5849/wjaf.11-042.

Oliver, W.W., Ryker, R.A. 1990. Ponderosa pine. In: R.M. Burns, B.H. Honkala, eds. 1990. *Silvics of North America* 1. Conifers. Agriculture Handbook 654, USDA Forest Service, Washington DC, USA, pp. 413–424.

R Core Team. 2024. R: a language and environment for statistical computing. R Foundation for Statistical Computing, Vienna, Austria. https://www.R-project.org. Accessed 27 Aug 2025.

Reynolds, R. T., Graham, R. T., Reiser, M. H. 1992. Management recommendations for the northern goshawk in thesouthwestern United States. *Gen. Tech. Rep. RM-GTR-217. Fort Collins, CO: USDA Forest Service, Rocky Mountain Forest and Range Experiment Station. 90 p*. https://research.fs.usda.gov/treesearch/6420.

Rhoades, P. R., T. S. Davis, W. T. Tinkham, and C. M. Hoffman. 2018. Effects of seasonality, forest structure, and understory plant richness on bee community assemblage in a southern rocky mountain mixed conifer forest. *Annals of the Entomological Society of America* 111 (5): 278–284. https://doi.org/10.1039/aesa/say021.

Riley, K.L., Grenfell, I.C., Finney, M.A., Shaw, J.D. 2021. TreeMap 2016: a tree-level model of the forests of the conterminous United States Circa 2016; Forest Service Research Data Archive: Fort Collins, CO, USA.

Ritter, S. M., C. M. Hoffman, M. A. Battaglia, and T. B. Jain. 2022. Restoration and fuel hazard reduction result in equivalent reductions in crown fire behavior in dry conifer forests. *Ecological Applications* 32 (7) : e2682. https://doi.org/10.1002/eap.2682.

Roussel, J., D. Auty, N. C. Coops, P. Tompalski, T. R. Goodbody, A. S. Meador, J. Bourdon, F. de Boissieu, and A. Achim. 2020. lidR: An R package for analysis of airborne laser scanning (ALS) data. *Remote Sensing of Environment* 251 : 112061. https://doi.org/10.1016/j.rse.2020.112061.

Roussel, J. 2025. lasR: fast and pipeable airborne LiDAR data tools. R package version 0.13.6, https://github.com/r-lidar/lasr. Accessed 25 Mar 2025.

Shepperd, W. D., Battaglia, M. A. 2002. *Ecology, silviculture, and management of Black Hills ponderosa pine*. Gen.Tech. Rep. RMRS-GTR-97. Fort Collins, CO: USDA Forest Service, Rocky Mountain ResearchStation. 112 p. https://research.fs.usda.gov/treesearch/4816.

Silva, C. A., Hudak, A. T., Vierling, L. A., Loudermilk, E. L., O'Brien, J. J., Hiers, J. K., Gonzalez-Benecke, C., Lee, H.,Falkowski, M. J., Khosravipour, A. 2016. Imputation of individual longleaf pine (Pinus palustris Mill.) tree attributesfrom fi eld and LiDAR data. *Canadian Journal of Remote Sensing* 42(5):554–573. https://doi.org/10.1080/07038992.2016.1196582.

Steel, Z. L., H. D. Safford, and J. H. Viers. 2015. The fire frequency-severity relationship and the legacy of fire suppression in California forests. *Ecosphere* 6 (1): 1–23. https://doi.org/10.1890/ES14-00224.1.

Stephens, S. L., M. A. Battaglia, D. J. Churchill, B. M. Collins, M. Coppoletta, C. M. Hoffman, J. M. Lydersen, M. P. North, R. A. Parsons, S. M. Ritter, et al. 2021. Forest restoration and fuels reduction: Convergent or divergent? *BioScience* 71:85–101. https://doi.org/10.1093/biosci/biaa134.

St-Onge, B. 2008. Methods for improving the quality of a true orthomosaic of Vexcel UltraCam images created usinga lidar digital surface model. In Proceedings of the Silvilaser 2008, Edinburgh, UK, 17–19 September 2008; pp. 555 562. https://chaireafd.uqat.ca/publication/articlePDF/SilviLaser2008St-Onge.pdf.

Swayze, N. C., and W. T. Tinkham. 2022. Application of unmanned aerial system structure from motion point cloud detected tree heights and stem diameters to model missing stem diameters. *MethodsX* 9:101729. https://doi.org/10.1016/j.mex.2022.101729.

Swayze, N. C., W. T. Tinkham, J. C. Vogeler, and A. T. Hudak. 2021. Influence of flight parameters on UAS-based monitoring of tree height, diameter, and density. *Remote Sensing of Environment* 263 : 112540. https://doi.org/10.1016/j.rse.2021.112540.

Tinkham, W. T., Mahoney, P. R., Hudak, A. T., Domke, G. M., Falkowski, M. J., Woodall, C. W., Smith, A. M. S. 2018. Applications of the United States Forest Inventory and Analysis dataset: a review and future directions. *CanadianJournal of Forest Research* 48:1–18. https://doi.org/10.1139/cjfr-2018-0196.

Tinkham, W. T., and N. C. Swayze. 2021. Influence of Agisoft Metashape parameters on UAS structure from motion individual tree detection from canopy height models. *Forests* 12 (2) : 250. https://doi.org/10.3390/f12020250.

Tinkham, W. T., and G. A. Woolsey. 2024. Influence of structure from motion algorithm parameters on metrics for individual tree detection accuracy and precision. *Remote Sensing* 16 : 3844. https://doi.org/10.3390/rs16203844.

Tinkham, W. T., M. A. Battaglia, and C. M. Hoffman. 2021. Evaluating long-term seedling growth across densities using Nelder plots and the Forest Vegetation Simulator (FVS) in the Black Hills, South Dakota, USA. *Forest Science* 67 (4): 380–388. https://doi.org/10.1093/forsci/fxab009.

Tinkham, W. T., N. C. Swayze, C. M. Hoffman, L. E. Lad, and M. A. Battaglia. 2022. Modeling the missing DBHs: Influence of model form on UAV DBH characterization. *Forests* 13 : 2077. https://doi.org/10.3390/f13122077.

Tinkham, W. T., Dickinson, Y., Hoff man, C. M., Battaglia, M. A., Ex, S., Underhill, J. 2017. Visualization ofheterogeneous forest structures following treatment in the southern Rocky Mountains. *Gen. Tech. Rep. RMRS-GTR-365. Fort Collins, CO: USDA Forest Service, Rocky Mountain Research Station. 72 p*. https://research.fs.usda.gov/treesearch/54887.

Tinkham, W.T., Battaglia, M.A., Woolsey, G.A. 2026. Uncrewed Aerial System imagery and collocated validation field plots from assessment of forest spatial pattern in Black Hills South Dakota, USA restoration treatments. Fort Collins, CO: USDA Forest Service Research Data Archive. https://doi.org/10.2737/RDS-2026-0003.

USDA Forest Service. 2009. *Timber Cruising Handbook*: Chapter 70 - DesignatingTimber for Cutting. In Forest Service Handbook: Renewable resources handbook (FSH 2409.12). Washington, DC:Author. Retrieved from https://www.usda.gov/guidance-documents/designating-timber-cutting/fs/forest-service-handbook-240912-70-timber-cruising-handbook.

Underhill, J. L., Y. Dickinson, A. Rudney, and J. Thinnes. 2014. Silviculture of the Colorado Front Range landscape restoration initiative. *Journal of Forestry* 112 (5): 484–493.

Wing, B. M., K. Boston, and M. W. Ritchie. 2019. A technique for implementing group selection treatments with multiple objectives using an airborne LiDAR-derived stem map in a heuristic environment. *Forest Science* 65 (2): 211–222. https://doi.org/10.1093/forsci/fxy050.

Yeo, B. J., and M. Stewart. 2000. Thinning *Pinus radiata* plantation by operator selection: 1. Effects on the residual forest. *Australian Forestry* 63 (4): 284–292. https://doi.org/10.1080/00049158.2000.10674843.

Young, D. J. N., J. T. Stevens, J. M. Earles, J. Moore, A. Ellis, A. L. Jirka, and A. M. Latimer. 2017. Long-term climate and competition explain forest mortality patterns under extreme drought. *Ecology Letters* 20:78–86. https://doi.org/10.1111/ele.12711.

Zhang, W., J. Qi, P. Wan, H. Wang, D. Xie, X. Wang, and G. Yan. 2016. An easy-to-use airborne LiDAR data filtering method based on cloth simulation. *Remote Sensing* 8 : 501. https://doi.org/10.3390/rs8060501.

Ziegler, J. P., C. M. Hoffman, W. T. Tinkham, R. A. Parsons, M. A. Battaglia, and J. Menakis. 2025. Impact of thinning strategy, surface fuel loading and burning conditions on fuel treatment efficacy in ponderosa pine dominated forests of the Southern Rocky Mountains. *Forest Science*. https://doi.org/10.1007/s44391-025-00034-8.

Publisher's Note Springer Nature remains neutral with regard to jurisdictional claims in published maps and institutional affiliations.

Authors and Affiliations

Wade T. Tinkham[1] · Mike A. Battaglia[1] · George A. Woolsey[2] · Lauren E. Lad[2] · Lance A. Asherin[1]

✉ Wade T. Tinkham
Wade.Tinkham@usda.gov

[1] Rocky Mountain Research Station, USDA Forest Service, 240 West Prospect Road, Fort Collins, CO 80526, USA

[2] Department of Forest and Rangeland Stewardship, Colorado State University, 1472 Campus Delivery, Fort Collins, CO 80523, USA